Supplementary Fig.1

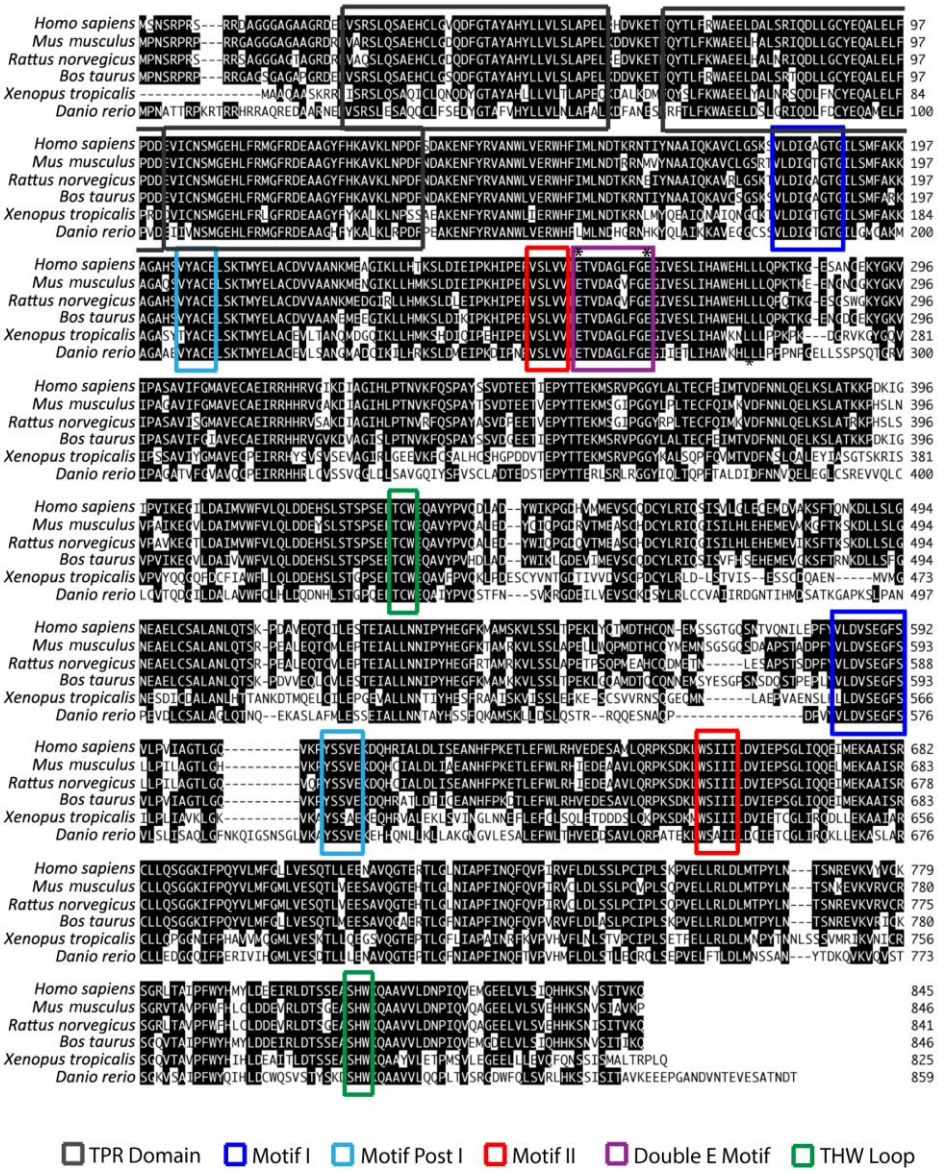

Supplementary Fig. 1. PRMT9 is conserved among species.

Vertebrate PRMT9 protein sequences from *Danio rerio* (NP_001124239.1), *Xenopus tropicalis* (NP_001135658.1), *Bos taurus* (NP_001092521.1), *Rattus norvegicus* (NP_001178528.1), *Mus musculus* (NP_001074709.1) and *Homo sapiens* (NP_612373.2) were aligned by Clustal W. Colored boxes indicate the conserved protein domains/motifs that have been identified as shown at the bottom of the figure. Shaded residues are identical in multiple species.

Supplementary Fig.2

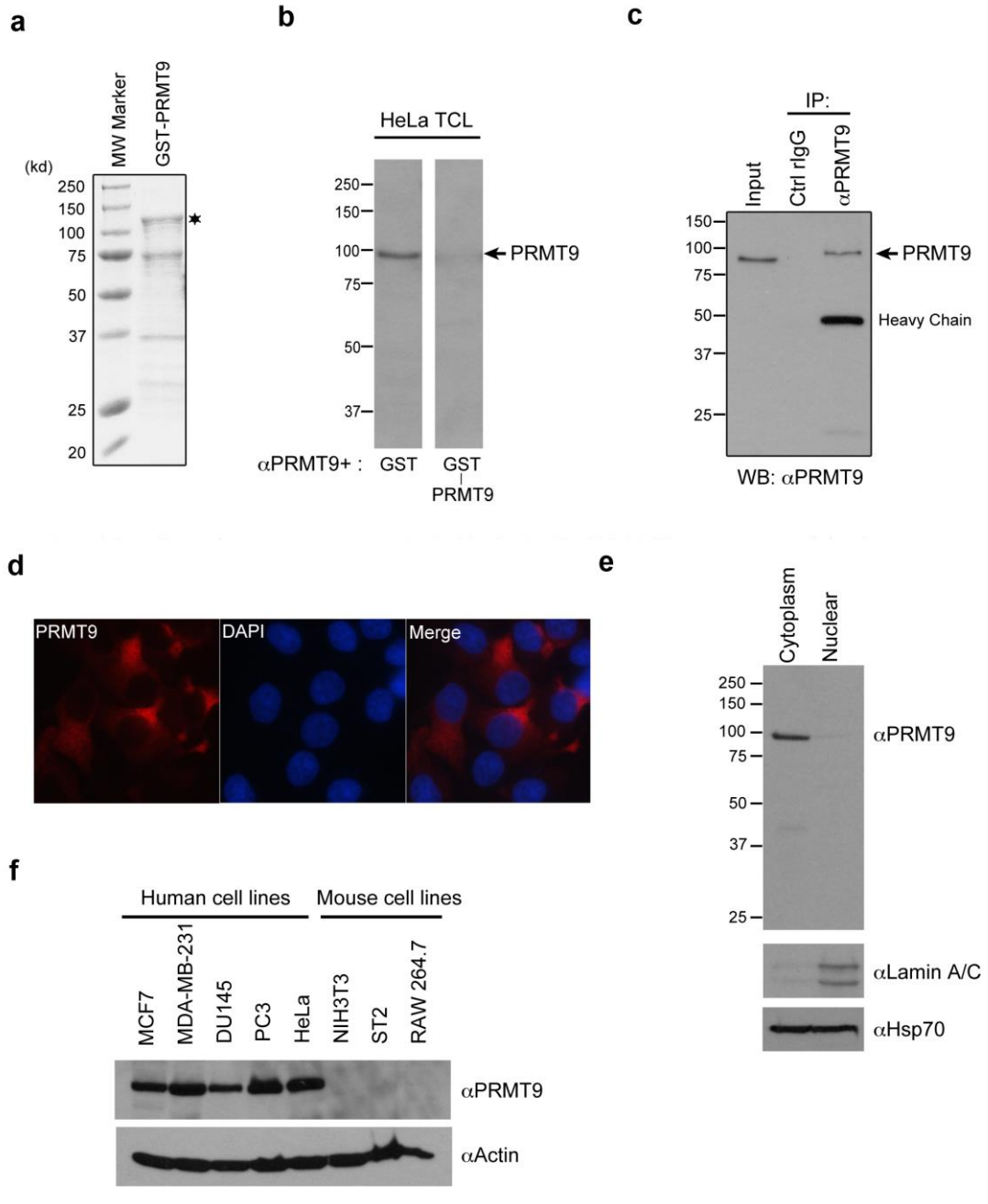

Supplementary Fig. 2. Characterization of mouse anti-PRMT9 monoclonal antibody.

(**a**) Expression and purification of GST-PRMT9. Recombinant protein was loaded on SDS-PAGE gel and stained with Coomassie blue. The asterisk indicates the position of the full length GST-PRMT9 protein.

(**b**) Characterization of PRMT9 antibody by western blot. 30 µg of HeLa cell lysate was loaded on SDS-PAGE gel and detected with αPRMT9 antibody or αPRMT9 antibody that has been neutralized by excessive amount of recombinant GST-PRMT9.

(**c**) Characterization of PRMT9 antibody by immunoprecipitation. 1 mg of HeLa cell lysate protein was immunoprecipitated with either rabbit control IgG or αPRMT9 antibody. The eluted samples were run on SDS-PAGE gel and detected by western blot using αPRMT9 antibody.

(**d**) Determination of PRMT9 subcellular localization by immunofluorescence. Immunofluorescence was performed in HeLa cells using αPRMT9 antibody at 1:1000 dilution, showing predominant cytoplamic localization of endogenous PRMT9. DAPI staining indicates the nucleus.

(**e**) PRMT9 mainly localizes in cytoplasm. Western blot of cytoplasmic and nuclear fractions of HeLa cells were probed with αPRMT9 monoclonal antibody, showing cytoplasmic localization of PRMT9. Lamin A/C expression is used as a marker of the nucleus.

(**f**) PRMT9 monoclonal antibody does not cross react with mouse PRMT9 protein. Total cell lysates from a panel of human cancer cell lines and mouse cell lines were detected for PRMT9 expression by western blotting. Results from both long and short exposure were shown. αActin blotting was shown as loading controls.

Supplementary Fig.3

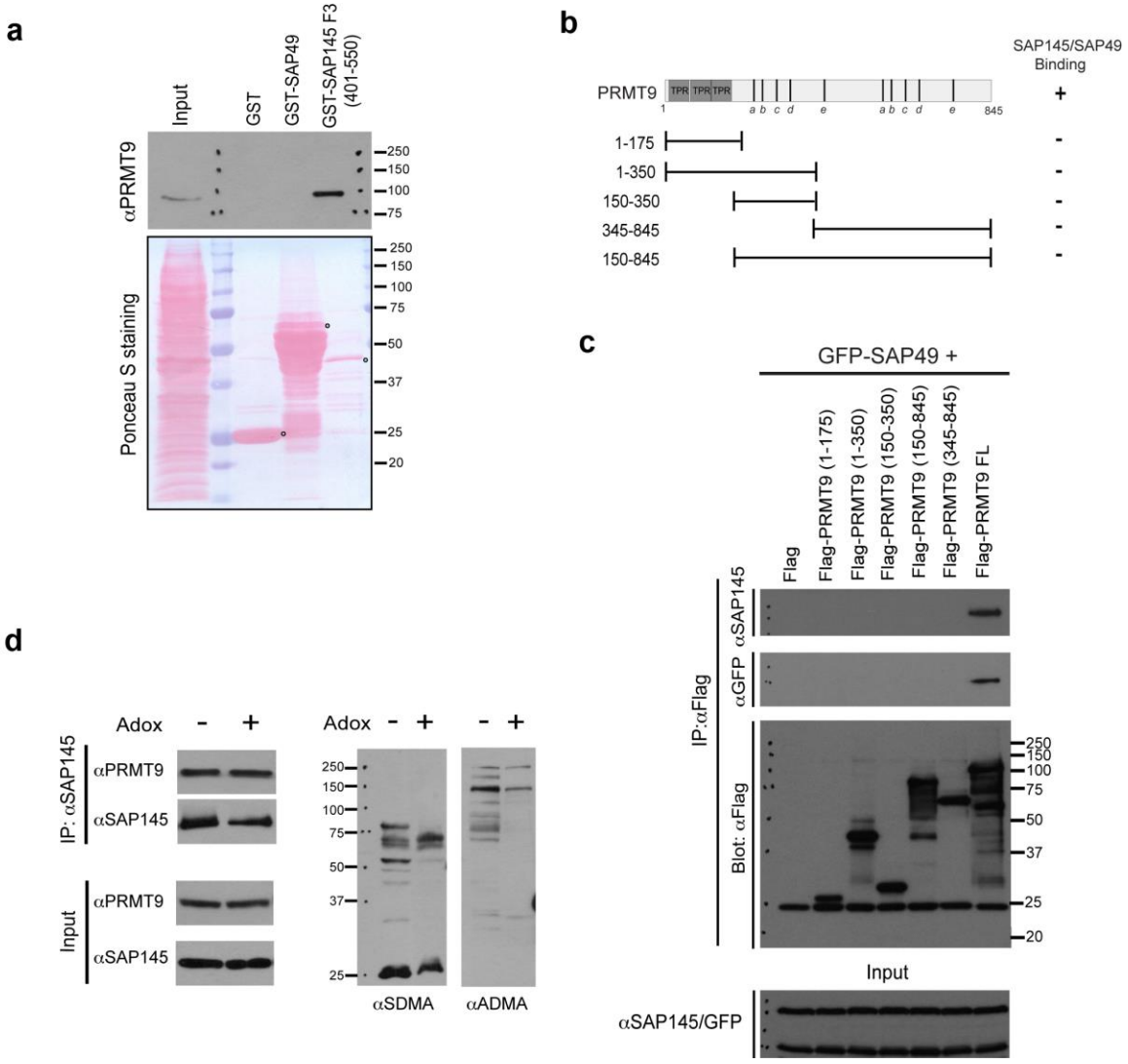

Supplementary Fig. 3. Further characterization of PRMT9-SAP145 interaction.

(**a**) SAP145, but not SAP49, interacts with PRMT9 directly. GST pull-down experiment was performed by incubating HeLa cell lysates with purified GST, GST-tag SAP49 and GST-SAP145 fragments F3. The pull-down samples were eluted and detected by western blotting using αPRMT9 antibody. The open circles indicate the positions of individual GST-tag proteins.

(**b**) A series of Flag-fusion truncations of PRMT9 were generated. The locations of the TPR domains and the identified motifs in methyltransferase domain are indicated. The graphic summary of the interactions observed in (**c**) is shown. a-e indicate signature PRMT motifs: a,

Motif I: VLD/EVGXGXG; b, Post I: V/IXG/AXD/E; c, Motif II: F/I/VDI/L/K; d, Motif III: LR/KXXG; e, THW loop.

(**c**) A coIP assay was performed in HeLa cells transfected with the different PRMT9 Flag-fusion vectors and GFP-SAP49. The cell lysates were immunoprecipitated with αFlag antibody and eluted samples were blotted with αGFP, αSAP145 and αFlag. Total cell lysates were detected with both αGFP and αSAP145 as input controls.

(**d**) Inhibition of methylation by AdOx does not affect PRMT9-SAP145 interaction. HeLa cells were treated with 20 μM of AdOx for 6 days before the immunoprecipitation was performed with the αSAP145 antibody. The eluted samples were detected with αSAP145 and αPRMT9 antibodies.

Supplementary Fig.4

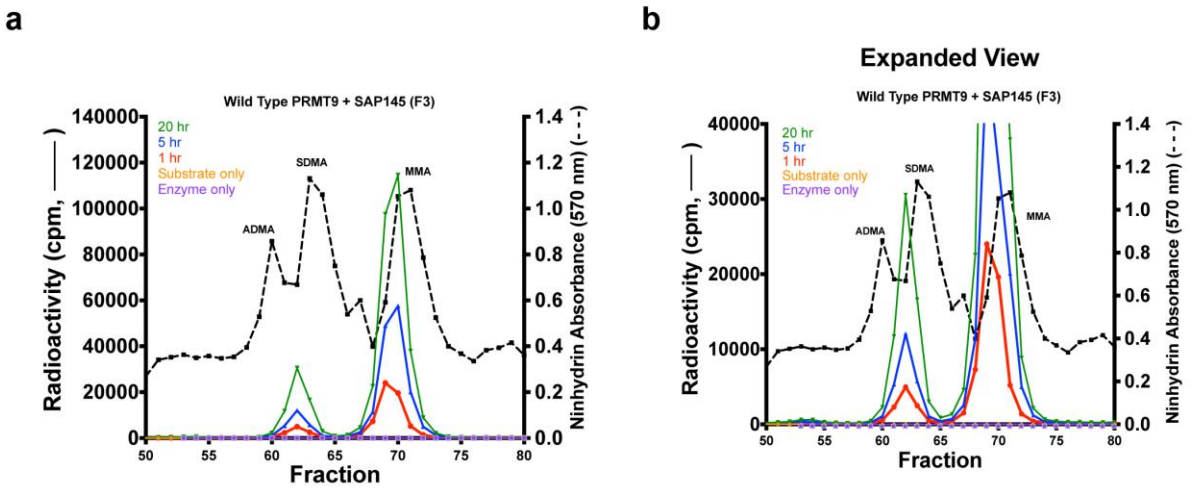

Supplementary Fig. 4. PRMT9 catalyzes symmetrical dimethylation of SAP145 in vitro. (**a**) PRMT9 symmetrically dimethylates SAP145 as analyzed by time-course amino acid analysis. Amino acid analysis of *in vitro* methylation products from three different time-course (1, 5 and 20 h) using GFP-PRMT9 as enzyme and GST-SF3B2 (401-550) fragment as substrate. Black dashed line indicates elution of nonradiolabeled standards. The radioactive peaks elute 1-2 min before the nonradiolabeled standards due to a tritium isotope effect [39]. (**b**) Expanded view of the amino acid analysis results from (**a**).

Supplementary Fig.5

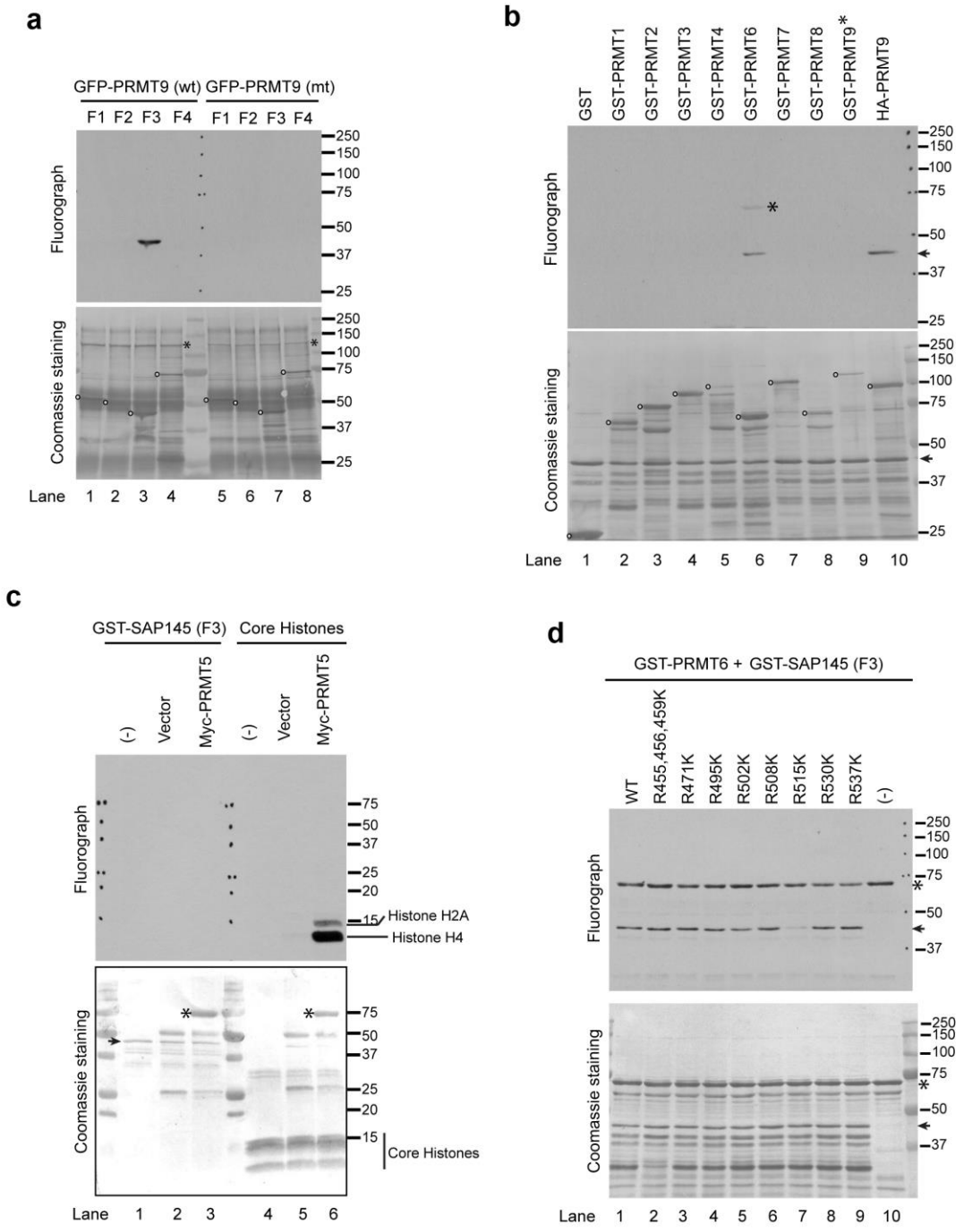

Supplementary Fig. 5. PRMT9 methylates SAP145 in vitro.

(**a**) PRMT9 methylates SAP145 fragment F3 (a.a. 401-550). The *in vitro* methylation assay was performed by incubating either wild type or enzymatic mutant GFP-PRMT9 (immunoprecipitated from HeLa cell lysates) with GST and GST-tag SAP145 fragments (F1- F4, as described in **Fig.**

3a,b). The reaction samples were run on a SDS-PAGE gel followed by exposure to x-ray film for 3 days. The membrane was then stained with Coomassie blue. The open circles indicate the substrates and the stars indicate the immunoprecipitated enzymes.

(**b**) In addition to PRMT9, PRMT6 can also methylate SAP145 *in vitro*. *In vitro* methylation was performed by incubating GST-tag recombinant enzymes and SAP145 fragment F3. HA-PRMT9 purified from sf21 cells was used as a positive control. GST-PRMT9 is inactive under these conditions. Coomassie blue staining displays the loading of the recombinant GST-tag enzymes (open circles) and substrates (arrow). The star on the fluorograph indicates the GST-PRMT6 automethylation signal.

(**c**) PRMT5 does not methylate SAP145. *In vitro* methylation was performed by incubating immunoprecipitated Myc-tag PRMT5 with either GST-SAP145 fragment F3 or purified core histones (positive control). In contrast to methylating Histone H2A and H4, PRMT5 does not methylate SAP145 fragment F3.

(**d**) Arginine 515 of SAP145 is methylated by PRMT6 *in vitro*. *In vitro* methylation assay was performed by incubating recombinant GST-PRMT6 with a series of Arg to Lys (R to K) mutants of SAP145 fragment F3 (see **Fig. 3a**,**b** for description). After exposure, the membrane was stained with coomassie blue to check the protein loading. Arrows indicate the positions of the substrates and stars indicate the position of the recombinant GST-PRMT6. Star on the fluorograph indicate the PRMT6 automethylation signals.

Supplementary Fig.6

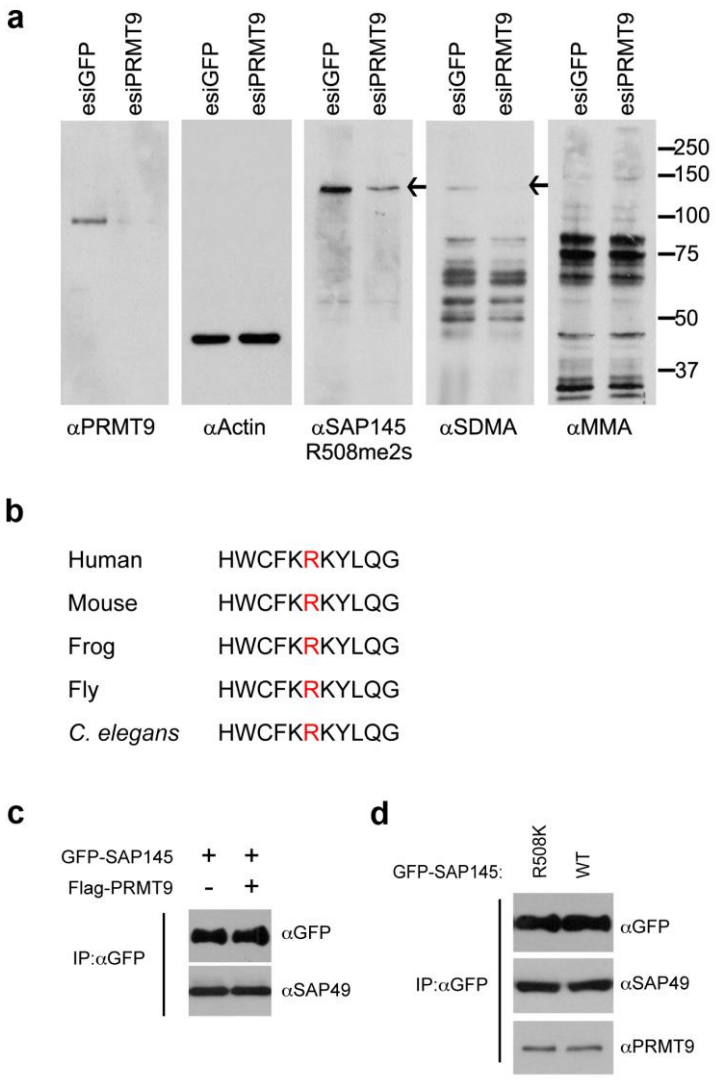

Supplementary Fig. 6. R508 methylation does not affect SAP145 interaction with SAP49 or PRMT9.

(**a**) Knockdown of PRMT9 decreases SAP145 R508 symmetrical dimethylation. HeLa cells were transiently transfected with either control esiGFP (esiRNA targeting GFP) or esiPRMT9 (esiRNA targeting PRMT9) for 48 hours. 30 μg of total cell lysates were subjected to western blotting and detected with αPRMT9, αActin, αSAP145 R508me2s, αSDMA, and αMMA antibodies. Arrows indicate the detection of SAP145 symmetrical dimethylation by αSAP145 R508me2s and αSDMA antibodies.

(**b**) Arginine 508 site of SAP145 is evolutionarily conserved among species. The conserved arginine is marked in red.

(**c**) Overexpression of PRMT9 does not affect SAP145-SAP49 interaction. Same immunoprecipitated samples as described in **Fig. 5d** were detected with αSAP49 antibody, by western blotting.

(**d**) SAP145 arginine methylation deficient mutant (R508K) can still interact with SAP49 and PRMT9. Same total cell lysates as described in **Fig. 5c** were immunoprecipitated with αGFP antibody, followed by western blotting with αGFP, αSAP49 and αPRMT9 antibodies.

Supplementary Fig.7

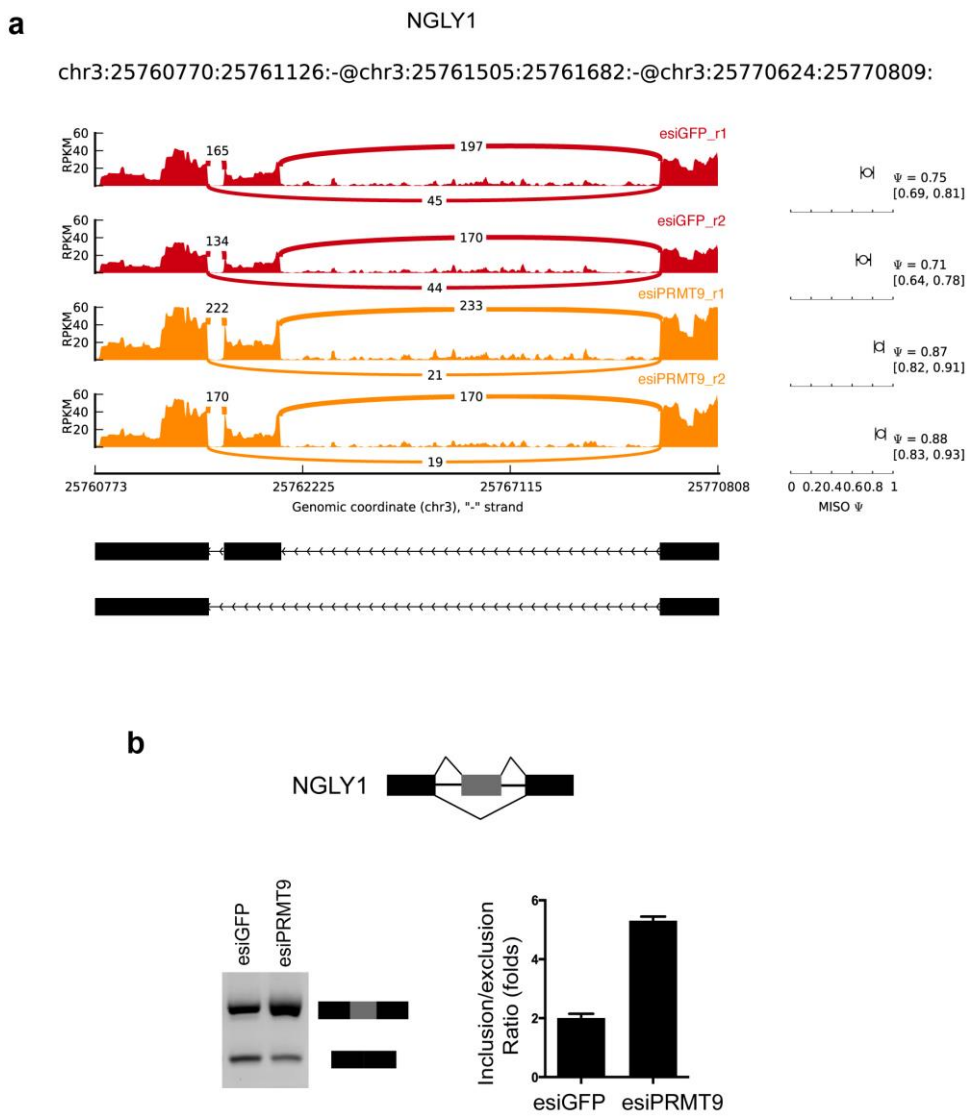

Supplementary Fig. 7. NGLY1 alternative splicing is regulated by PRMT9.

(**a**) RNA-seq read coverage across NGLY1 exon 10 to exon 12 from esiGFP control and esiPRMT9 knockdown HeLa cells. MISO PSI (Ψ) values and 95% confidence intervals were shown at right.

(**b**) Validation of exon exclusion of NGLY1 exon 11 in response to PRMT9 knockdown. RT-PCR experiments were performed using RNA extracted from esiGFP control and esiPRMT9 transfected HeLa cells with primers located on exon 10 and exon 12 (left panel). The PCR products were quantified by densitometric analysis. Inclusion vs exclusion ratio was calculated. Error bars represent standard deviation calculated from three independent experiments (right panel).

Supplementary Fig. 8 Full blots for figures in the main text

Fig. 2b

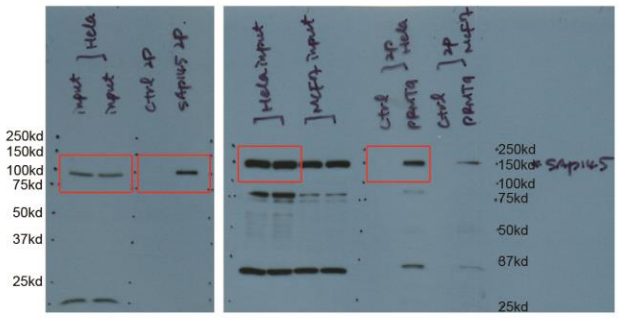

Fig. 2c

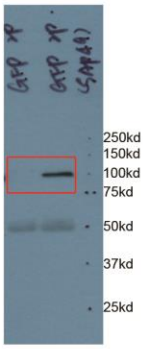

Fig. 2d

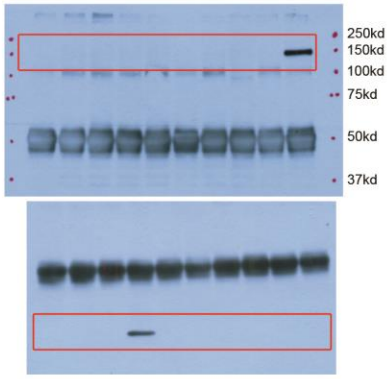

Fig. 3b

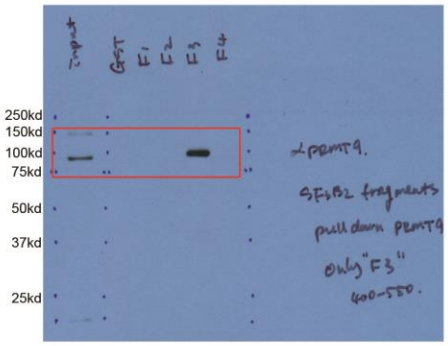

Fig. 3d

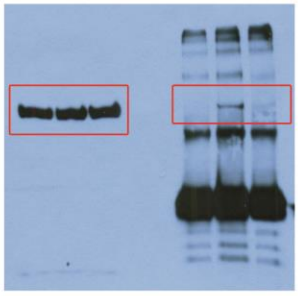

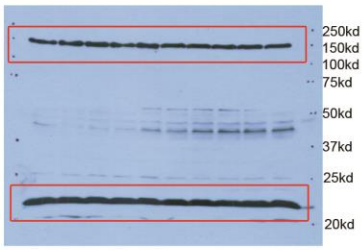

Fig. 4a

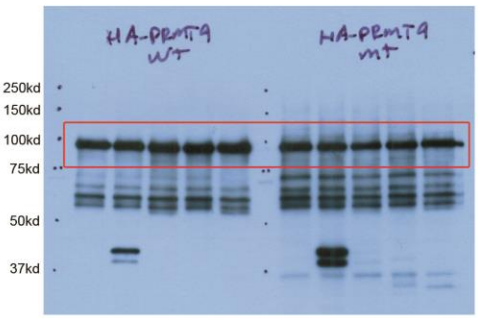

Fig. 5c

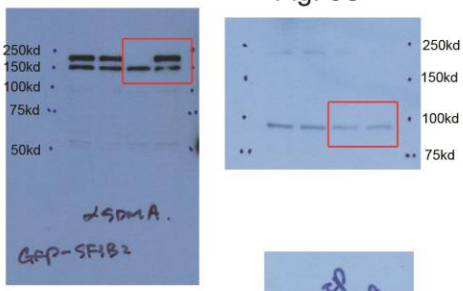

Fig. 5d

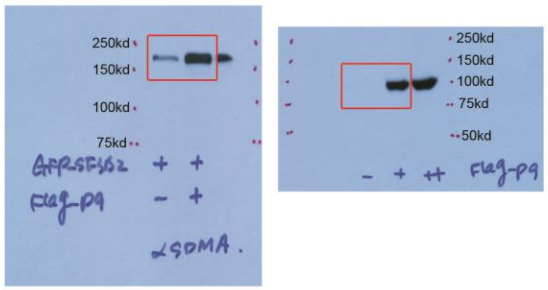

Fig. 5e

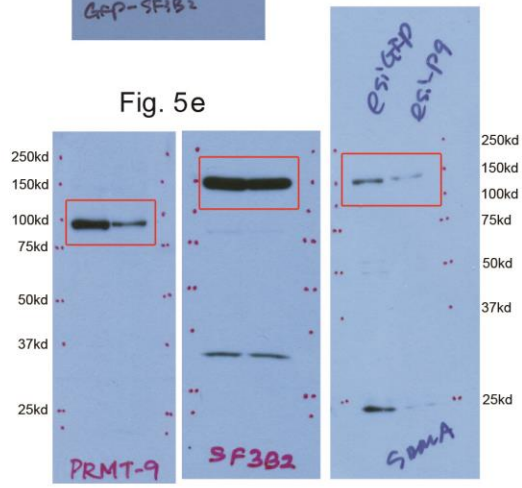

Supplementary Fig. 8 Full blots for figures in the main text, continued

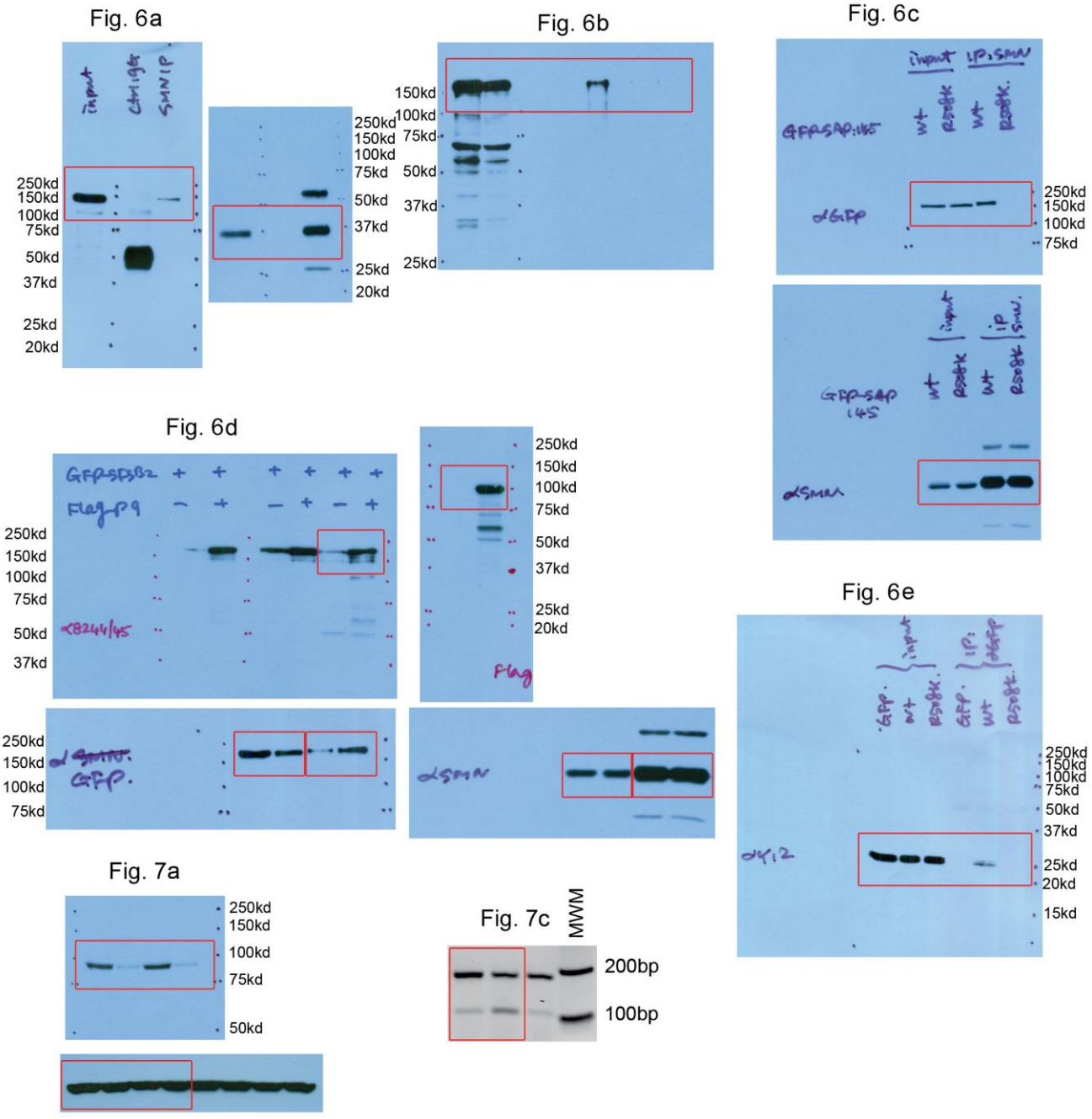

Table 1. PRMT9 regulated alternative splicing identified by RNA-Seq

type	gene	loci	Mean-PSI esiGFP	Mean-PSI esiPRMT9	PSI-Diff	Mean-BF
MXE	SNHG6	chr8:67834349-67837672	0.39	0.465	-0.075	7.57633E+11
MXE	PSMA6;KIAA0391	chr14:35779946-35786682	0.55	0.64	-0.09	1448263.703
MXE	UQCRB	chr8:97243360-97244002	0.205	0.505	-0.3	5.55212E+11
A3SS	NUSAP1;NA	chr15:41641296-41643327	0.76	0.865	-0.105	6345745.785
A3SS	PKD1	chr16:2155323-2155866	0.09	0.24	-0.15	3384.29
A3SS	SERBP1	chr1:67889883-67890571	0.255	0.345	-0.09	2.50103E+11
A3SS	GNB2L1	chr5:180663929-180665099	0.43	0.555	-0.125	5.00119E+11
A3SS	TRIM41	chr5:180659659-180660763	0.35	0.79	-0.44	12.0125
A3SS	PRICKLE4;TOMM6	chr6:41756970-41757634	0.265	0.365	-0.1	1254817028
A3SS	WSB1	chr17:25633808-25636298	0.615	0.855	-0.24	2.50032E+11
A3SS	CELF1	chr11:47487489-47493743	0.56	0.715	-0.155	5E+11
A3SS	LINC00473	chr6:166362743-166401017	0.22	0.15	0.07	4598939182
A5SS	BACE2	chr21:42613746-42615437	0.825	0.71	0.115	7.50194E+11
A5SS	SNORD101;RPS12	chr6:133136111-133137702	0.245	0.455	-0.21	1.00E+12
A5SS	RPL12	chr9:130213083-130213684	0.015	0.075	-0.06	1.00E+12
A5SS	PABPC4	chr1:40035674-40037021	0.06	0.17	-0.11	4464592.685
A5SS	OCIAD1	chr4:48853823-48863834	0.385	0.63	-0.245	139017439.4
A5SS	IFI35	chr17:41165284-41165679	0.935	0.62	0.315	60.6475
A5SS	PARK7	chr1:8021714-8022935	0.405	0.54	-0.135	2.50634E+11
A5SS	SLC25A3	chr12:98989211-98991813	0.07	0.205	-0.135	1166477.268
A5SS	OCIAD1	chr4:48853823-48863834	0.37	0.61	-0.24	2.50004E+11
RI	NONO	chrX:70517686-70518358	0.055	0.13	-0.075	3.10669E+11
RI	KDM3A	chr2:86718264-86719839	0.165	0.07	0.095	2.5001E+11
RI	NDUFS2	chr1:161183654-161184184	0.07	0.19	-0.12	1.00E+12

RI	HLTF	chr3:148747904-148750159	0.7	0.605	0.095	5E+11
RI	RABGGTB	chr1:76255637-76255959	0.55	0.35	0.2	2.5222E+11
RI	EEF1A1	chr6:74227753-74228333	0.055	0.135	-0.08	2.50334E+11
RI	NDUFS2	chr1:161183654-161184185	0.07	0.19	-0.12	1.00E+12
RI	TAF1D	chr11:93469860-93470405	0.15	0.095	0.055	5.32578E+11
RI	TGFBI	chr5:135382024-135382704	0.1	0.235	-0.135	214098.83
RI	SLC25A3	chr12:98987753-98989626	0.07	0.17	-0.1	1.00E+12
RI	KDM3A	chr2:86716643-86718180	0.19	0.1	0.09	218490.055
RI	DDX39B	chr6:31500557-31503262	0.225	0.365	-0.14	23193.6125
RI	FAM200B	chr4:15687859-15692070	0.715	0.525	0.19	156691493.3
type	**gene**	**loci**	**Mean-PSI esiGFP**	**Mean-PSI esiPRMT9**	**PSI-Diff**	**Mean-BF**
SE	PDK1	chr2:173431584-173435552	0.625	0.415	0.21	5E+11
SE	EIF4A2	chr3:186505592-186507685	0.35	0.28	0.07	5E+11
SE	RPL5	chr1:93299102-93300470	0.01	0.06	-0.05	8.96759E+11
SE	ESYT2	chr7:158542414-158552177	0.61	0.485	0.125	84.8075
SE	BCOR	chrX:39930412-39931602	0.63	0.5	0.13	6.80036E+11
SE	RPS18	chr6:33240405-33243660	0.1	0.325	-0.225	2.53345E+11
SE	AKAP13	chr15:86198648-86207986	0.37	0.15	0.22	129547714.9
SE	WAC	chr10:28879649-28897360	0.905	0.965	-0.06	5E+11
SE	KRAS	chr12:25362845-25378548	0.11	0.045	0.065	1689.9475
SE	C17orf76-AS1	chr17:16342641-16343567	0.21	0.315	-0.105	5E+11
SE	UGP2	chr2:64068098-64083567	0.26	0.43	-0.17	11751.8175
SE	TRMU	chr22:46733676-46742441	0.65	0.44	0.21	1723.5925
SE	FLNB	chr3:58116468-58118658	0.495	0.22	0.275	39.075
SE	BAG1	chr9:33261167-33262700	0.06	0.15	-0.09	2.52386E+11
SE	HNRPDL	chr4:83346036-83347190	0.54	0.845	-0.305	1.00E+12
SE	CD44	chr11:35240863-35253949	0.865	0.945	-0.08	1104.3325
SE	PIKFYVE	chr2:209138308-	0.62	0.33	0.29	54.435

		209150657				
SE	NIN	chr14:51221585-51226575	0.49	0.33	0.16	342993.52
SE	AL590482.1	chr6:166354254-166401017	0.56	0.79	-0.23	1.00E+12
SE	AL590482.1	chr6:166354254-166401017	0.455	0.565	-0.11	2777.1425
SE	WARS	chr14:100835595-100842597	0.355	0.735	-0.38	71.2425
SE	KTN1	chr14:56139647-56142636	0.385	0.235	0.15	7.50002E+11
SE	UQCRB	chr8:97243360-97244002	0.1	0.255	-0.155	5.01733E+11
SE	C17orf76-AS1	chr17:16342641-16343567	0.155	0.265	-0.11	5.05874E+11
SE	EEF1B2	chr2:207025312-207026196	0.05	0.305	-0.255	1.00E+12
SE	C17orf76-AS1	chr17:16342641-16343567	0.22	0.31	-0.09	5.00005E+11
SE	SH3D19	chr4:152065202-152069074	0.11	0.035	0.075	11052.275
SE	EDEM1	chr3:5249778-5252983	0.82	0.605	0.215	3825.795
SE	PTP4A2	chr1:32384848-32403643	0.22	0.355	-0.135	356.8325
SE	EEF1D	chr8:144672000-144679585	0.315	0.635	-0.32	655.545
SE	ATP13A3	chr3:194123406-194134568	0.58	0.465	0.115	3950496.895
SE	NGLY1	chr3:25760770-25770809	0.73	0.875	-0.145	96.065
SE	DCAF6	chr1:167973771-168012378	0.965	0.76	0.205	7.69542E+11
SE	MON2	chr12:62959017-62960230	0.775	0.435	0.34	135.3625